EVIDENTIAL FEDERATED LEARNING FOR SKIN LESION IMAGE CLASSIFICATION

Rutger Hendrix
Department of Electrical, Electronic
and Computer Engineering
University of Catania, Italy
rutger.hendrix@phd.unict.it

Federica Proietto Salanitri
Department of Electrical, Electronic
and Computer Engineering
University of Catania, Italy
federica.proiettosalanitri@unict.it

Concetto Spampinato
Department of Electrical, Electronic
and Computer Engineering
University of Catania, Italy
concetto.spampinato@unict.it

Simone Palazzo
Department of Electrical, Electronic
and Computer Engineering
University of Catania, Italy
simone.palazzo@unict.it

Ulas Bagci
Machine & Hybrid Intelligence Lab
Department of Radiology
Northwestern University, USA
ulas.bagci@northwestern.edu

ABSTRACT

We introduce *FedEvPrompt*, a federated learning approach that integrates principles of evidential deep learning, prompt tuning, and knowledge distillation for distributed skin lesion classification. FedEvPrompt leverages two sets of prompts: *b-prompts* (for low-level basic visual knowledge) and *t-prompts* (for task-specific knowledge) prepended to frozen pre-trained Vision Transformer (ViT) models trained in an evidential learning framework to maximize class evidences. Crucially, knowledge sharing across federation clients is achieved only through knowledge distillation on attention maps generated by the local ViT models, ensuring enhanced privacy preservation compared to traditional parameter or synthetic image sharing methodologies. FedEvPrompt is optimized within a round-based learning paradigm, where each round involves training local models followed by attention maps sharing with all federation clients. Experimental validation conducted in a real distributed setting, on the ISIC2019 dataset, demonstrates the superior performance of FedEvPrompt against baseline federated learning algorithms and knowledge distillation methods, without sharing model parameters. In conclusion, FedEvPrompt offers a promising approach for federated learning, effectively addressing challenges such as data heterogeneity, imbalance, privacy preservation, and knowledge sharing.

Keywords Prompt Tuning · Knowledge Distillation · Uncertainty

1 Introduction

In recent decades, deep learning has played a leading role in medical image analysis, including skin lesion classification. However, most of the existing methods rely on centralized learning, assuming data uniformity and accessibility, which often does not align with the reality of decentralized and privacy-sensitive clinical settings. This disparity not only limits progress in the field, but also exacerbates inequalities, with wealthier regions having a data advantage over poorer areas, leading to disparities in model performance and clinical support. Federated learning (FL) emerges as a promising

solution to this challenge, enabling model training across distributed devices while preserving data privacy. Methods like FedAvg McMahan et al. [2017] and FedProx Li et al. [2020] have addressed issues such as non-i.i.d. data and system heterogeneity, yet they still face obstacles, particularly in scenarios with class imbalances and data heterogeneity. Evidential Deep Learning (EDL) Sensoy et al. [2018a] has found adoption in FL to handle these limitations in medical data, thereby enhancing model confidence and reliability, crucial for clinical applications. For example, the recent work on uncertainty-aware aggregation of federated models for diabetic retinopathy classification demonstrates its efficacy in improving model performance and reliability Wang et al. [2023].

Furthermore, the scarcity of data poses an additional significant challenge, often leading to model overfitting and suboptimal federation performance. Recent techniques like learnable prompting Li and Liang [2021], particularly effective in low-data regimes, offer a promising solution by facilitating personalized model tuning across distributed clients Li et al. [2023]. Nonetheless, privacy concerns persist, particularly due to the sharing and aggregation of model parameters, which poses the risk of reconstructing training images, as demonstrated by recent studies Zhang et al. [2023], Geiping et al. [2020], Zhu et al. [2019]. To mitigate these concerns, one strategy involves sharing suitably-constructed synthetic data generated through generative models Pennisi et al. [2024]. Yet, the use of generative models carries its own risks, potentially incorporating and synthesizing sensitive training samples, thus exacerbating privacy concerns. We here propose FedEvPrompt, a novel approach that integrates principles of evidential deep learning, prompt tuning, and knowledge distillation to address existing limitations comprehensively. FedEvPrompt leverages prompts prepended to pre-trained ViT models trained in an evidential learning setting, maximizing class evidence. Knowledge sharing across federation clients is achieved only through knowledge distillation on attention maps generated by ViT models, which offers greater privacy preservation compared to sharing parameters or synthetic images, as it lacks pixel-level details and reconstructive qualities. While our approach maintains a high level of abstraction for minimizing privacy leaks, it also provides richer information than average logits, as in FedDistill Seo et al. [2022], or prototypes, as in FedProto Tan et al. [2022]. Thus, FedEvPrompt represents a principled way to share insights into the decision-making process of local models for enhanced federated performance, as demonstrated by the results achieved on a real-word distributed setting for skin lesion classification.

2   Background Evidential Learning

Deep Learning methods often use softmax activation in the output layers to perform classification. However, softmax outputs can be biased to training data, failing to predict with low certainty even for samples far from the distribution Ståhl et al. [2020]. In contrast to the additivity principle in probability theory, Dempster-Shafer theory describes that the sum of belief can be less than 1. Its remainder is then attributed to uncertainty.

In a frame of K mutually exclusive singletons (e.g., class labels), each singleton $k \in [K]$ is assigned a belief mass b_k, and an overall uncertainty mass u. The sum of these $K + 1$ mass values is constrained by $u + \sum_{k=1}^{K} b_k = 1$, with $u \geq 0, b_k \geq 0, \forall k \in [K]$. The belief mass is determined by the evidence supporting each singleton, reflecting the level of support gathered from data. The uncertainty is inversely proportional to the total amount of evidence, with uncertainty equal to 1 for a total lack of evidence. A belief mass assignment corresponds to a Dirichlet distribution with parameters $\alpha_k = e_k + 1$, where e_k denotes the derived evidence for the k-th singleton. This choice of Dirichlet distribution is motivated by its role as a conjugate prior to the categorical distribution, and is defined as:

$$\mathrm{Dir}(p, \alpha) = \frac{\Gamma(S)}{\prod_{k=1}^{K} \Gamma(\alpha_k)} \prod_{k=1}^{K} p_k^{\alpha_k - 1}, \quad \alpha_k > 0$$

where p denotes a probability mass function, K denotes the number of classes, $\alpha = [\alpha_1, \ldots, \alpha_K]$ are the Dirichlet parameters related to the evidence, $\Gamma(\cdot)$ denotes the gamma function, and $S = \sum_{k=1}^{K} \alpha_k$ is termed the Dirichlet strength.

From the parameters of this Dirichlet distribution, the belief b_k and the uncertainty u are derived as:

$$b_k = \frac{\alpha_k - 1}{S}, \quad u = \frac{K}{S}$$

When considering an opinion, the expected probability $\hat{p}_k$ of the k-th singleton equates to the mean of the corresponding Dirichlet distribution, calculated by:

$$\hat{p}_k = \frac{\alpha_k}{S}$$

Although this modeling of second-order probabilities and uncertainty enables the computation of different types of uncertainties, this work only considers classical vacuity uncertainty (u).

Evidential Deep Learning (EDL) aims to quantify these uncertainties in the predictions, using a single deterministic neural network. The model learns evidence from the logit layer, typically applying non-negative functions like ReLU to obtain these values. With these minimal changes, EDL models can be trained by minimizing losses such as evidential mean squared error (MSE) loss to form the multinomial opinions for K-class classification of a given sample i as a Dirichlet distribution. Following Sensoy et al. [2018b], the evidential MSE loss for sample i can be interpreted as:

$$\mathcal{L}_i(\Theta) = \int \left[(\mathbf{y}_i - \mathbf{p}_i)^T (\mathbf{y}_i - \mathbf{p}_i) \right] \mathrm{Dir}(\mathbf{p}_i, \alpha_i) d\mathbf{p}_i$$

$$= \sum_{k=1}^{K} \mathbb{E} \left[y_{i,k}^2 - 2 y_{i,k} y_{i,k} + p_{i,k}^2 \right]$$

where $\mathbf{y}_i = (y_{i,1}, \dots, y_{i,K})$ and $\mathbf{p}_i = (p_{i,1}, \dots, p_{i,K})$ are vectors of true and predicted probabilities, and $\alpha_i = (\alpha_{i,1}, \dots, \alpha_{i,K})$ are the Dirichlet parameters.

Using the identity $\mathbb{E}\left[p_{i,k}^2 \right] = \mathbb{E}\left[p_{i,k} \right]^2 + \mathrm{Var}(p_{i,k})$, the loss can be rewritten as:

$$\mathcal{L}_i(\Theta) = \sum_{k=1}^{K} \left((y_{i,k} - \mathbb{E}\left[p_{i,k} \right])^2 + \mathrm{Var}(p_{i,k}) \right)$$

$$= \sum_{k=1}^{K} \left(\left(y_{i,k} - \frac{\alpha_{i,k}}{S_k} \right)^2 + \frac{\alpha_{i,k}(S_i - \alpha_{i,k})}{S_i^2(S_i + 1)} \right)$$

where S_i is the total Dirichlet strength for sample i.

To avoid generating misleading evidence for incorrect labels, a Kullback-Leibler (KL) divergence regularization term is used, reducing total evidence to zero for incorrectly classified samples. The KL term is defined as:

$$\mathcal{L}_{KL} = \mathrm{KL}\left[\mathrm{Dir}(p_i \mid \widetilde{\alpha}_i) \| \mathrm{Dir}(p_i \mid \mathbf{1}) \right]$$

$$= \log \left(\frac{\Gamma\left(\sum_{k=1}^{K} \widetilde{\alpha}_{i,k} \right)}{\Gamma(K) \prod_{k=1}^{K} \Gamma(\widetilde{\alpha}_{i,k})} \right) + \sum_{k=1}^{K} (\widetilde{\alpha}_{i,k} - 1) \left(\psi(\widetilde{\alpha}_{i,k}) - \psi\left(\sum_{k=1}^{K} \widetilde{\alpha}_{i,j} \right) \right)$$

where $\widetilde{\alpha}_i$ are the Dirichlet parameters after the removal of non-misleading evidence defined as $\widetilde{\alpha} = y + (1 - y) \odot \alpha$, $\mathrm{KL}[.\|.]$ denotes the Kullback-Leibler divergence operator, and $\psi(.)$ is the digamma function Sensoy et al. [2018b]. The final **evidential loss** $\mathcal{L}_\epsilon$ results in:

$$\mathcal{L}_\epsilon = \mathcal{L}_i + \mathcal{L}_{KL}$$

3 Methodology

We introduce FedEvPrompt, our federated learning paradigm, which leverages prompt evidential learning and knowledge distillation on ViT attention maps for enabling effective knowledge aggregation across federated clients. The overall learning strategy is described in Fig. 1.

FedEvPrompt is based on a pre-trained ViT model, kept frozen across all clients within the federation. Upon the fixed backbone, prompts are prepended on each client model and optimized using local data. Each client also computes attention maps (through attention rollout mechanism Abnar and Zuidema [2020]) for each class and shares a subset of them with the federation. The attention maps by all clients form our *uncertainty-aware attention buffer* that is used for knowledge distillation during prompt learning.

Learning is organized in rounds: at each round, federation clients carry out different local training epochs for prompt optimization through a combination of evidential loss for learning class evidence and knowledge distillation loss on the per-class attention maps present within the buffer. At the end of training round, each client identifies its M most informative attention maps for each class and updates the buffer.

More in detail, each client employs a frozen ViT, as the backbone, with two sets of prompts *b-prompts* and *t-prompts*. Each prompt is associated with a specific attention layer, with the *b-prompts* (basic prompts) prepended to layers with low-level feature representation and the *t-prompts* (task-specifc prompts) to deeper layers with high-level feature
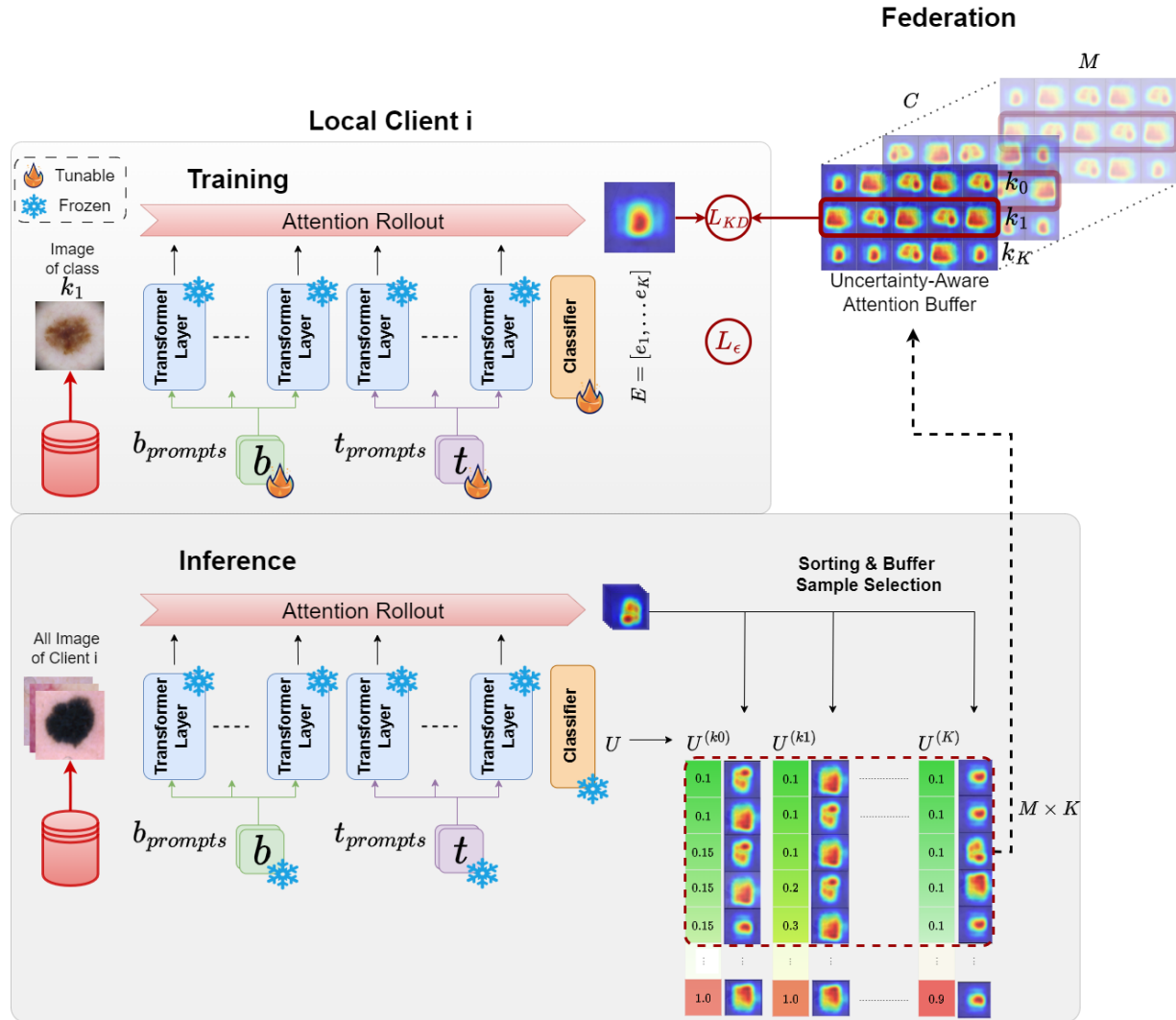
Figure 1: **Overview of FedEvPrompt**. During a round of **Training (top)**, local data is used to optimize *b-prompts*, encoding general visual features, and *t-prompts*, encoding task-specific information, prepended to a frozen ViT encoder. Optimization is carried out by minimizing evidential loss ($\mathcal{L}_\epsilon$) and a knowledge distillation loss ($\mathcal{L}_{\mathcal{KD}}$) between local attention maps and those of the federation available in the *uncertainty-aware attention buffer*. After a round of training at **Inference (bottom)**, the client identifies, for each class K, its M most informative attention rollout maps (sorted by lowest uncertainty) to contribute to the federated *uncertainty-aware attention buffer*.

representation. The parameters of the prompts are incorporated through pre-fix tuning. Let's denote the output of the i_{th} attention layer as h_i with $i \in 1 \cdots H$ where H is the number of attention layers. The prepended parameters for the key and value inputs, denoted as pr_k and pr_v respectively, are introduced as follows:

$$MSA(h_Q, [pr_k^{(i)}; h_K], [pr_v^{(i)}; h_V]) \tag{1}$$

where h_Q, h_K, and h_V represent the query, key, and value outputs from the previous layer, respectively. The prepended prompts $pr_k^{(i)}$ and $pr_v^{(i)}$ are *b-prompts* to the first l layers, and *t-prompts* to the last $H - l$ layers. The two sets of prompts undergo distinct optimization strategies: *b-prompts* require slower adaptation since the frozen backbone (ViT) has already grasped general visual features. Conversely, *t-prompts* necessitate faster adjustments to accommodate varying data distributions. Consequently, $\mu_1 < \mu_2$, where μ_1 and μ_2 denote the learning rates for the *b-prompts* and *g-prompts* optimizers, respectively. Both set of prompts are optimized by minimizing an overall loss $\mathcal{L}_G$ that includes an evidential loss term $\mathcal{L}_\epsilon$ and a knowledge distillation loss term $\mathcal{L}_{\mathcal{KD}}$ on the shared attention map buffer A:

$$\mathcal{L}_G = \mathcal{L}_\epsilon + \lambda \mathcal{L}_{\mathcal{KD}} \tag{2}$$

where $\lambda = 1e^{-6}$ is a parameter controlling the balance between the two terms.

3.1 Evidential loss

Our method is based on evidential learning, i.e., the classification model outputs evidences $E = [e_1, \ldots, e_K]$, with K categorical class elements (number of classes). The Dirichlet distribution characterizes the likelihood of each discrete probability value within a set of possible probabilities. It is parameterized by a vector of K elements (classes), $\boldsymbol{\alpha} = [\alpha_1, \ldots, \alpha_K]$, defined as $\alpha_k = e_k + W_k$, with e_k being the model evidence for class k, and W_k the prior weight for that class. Classical EDL assumes a uniform Dirichlet (Dir(1)) distribution as a prior, i.e., $\boldsymbol{W} = \langle 1, 1, \ldots, 1 \rangle$. The uncertainty for the ith input sample is then estimated as $u_i = \frac{K}{S}$, with S being the total Dirichlet strength $S = \sum_{k=1}^{K} \alpha_k$. Due to the strong class imbalance typical in federated learning settings, we change the uniform evidential prior to a skewed distribution, weighted by class frequency:

$$\alpha_k = e_k + W_k \quad \text{with} \quad W_k = \frac{K}{K-1}\left(1 - \frac{N_k}{N}\right) \tag{3}$$

such that $\sum_{k=1}^{K} W_k = K$.

Prompt parameters are finally optimized by minimizing the evidential loss defined in Sensoy et al. [2018b] as a combination of MSE and KL divergence. Given the ith input sample, the one-hot-encoded vector y_i of its class label k, and its expected probabilities p_i, the **evidential loss** $\mathcal{L}_\epsilon$ is computed as:

$$\mathcal{L}_\epsilon(\boldsymbol{\theta}) = \mathbb{E}_{\mathbf{p} \sim \text{Dir}(\boldsymbol{\alpha})}\left[(y_i - p_i)^T(y_i - p_i)\right] + \lambda_{KL} D_{KL}(\text{Dir}(p_i|\widetilde{\alpha}_i)||\text{Dir}(p_i|\mathbf{w}_i)) \tag{4}$$

with $\lambda_{KL} = min(1, t/10)$ being an annealing factor applied to gradually increase the regularization impact with the number of epochs t.

In order to let the evidence for incorrect classes shrink to the weighted prior values $\mathbf{W}$, the KL divergence loss term minimizes the distributional difference between $\mathbf{W}$ and misleading evidence $\widetilde{\boldsymbol{\alpha}}$, formulated as $\widetilde{\boldsymbol{\alpha}} = y \cdot \mathbf{w} + (1 - y) \odot \boldsymbol{\alpha}$. Given the weighted prior distribution $\mathbf{W} = \text{Dir}(\mathbf{p}|\mathbf{w})$ and $P = \text{Dir}(\mathbf{p}|\widetilde{\alpha})$, the general KL divergence form for the Dirichlet distribution Proof: becomes:

$$
\begin{aligned}
D_{KL}(\text{Dir}(p|\widetilde{\alpha})||\text{Dir}(p|\mathbf{w})) &= \log\left(\frac{\Gamma\left(\sum_{k=1}^{K}\widetilde{\alpha}_k\right)}{\Gamma\left(\sum_{k=1}^{K}w_k\right)}\right) + \sum_{k=1}^{K}\log\left(\frac{\Gamma(w_k)}{\Gamma(\widetilde{\alpha}_k)}\right) + \\
\sum_{k=1}^{K}(\widetilde{\alpha}_k - w_k) \cdot \left[\psi(\widetilde{\alpha}_k) - \psi\left(\sum_{k=1}^{K}\widetilde{\alpha}_k\right)\right] &= \log\left(\frac{\Gamma\left(\sum_{k=1}^{K}\widetilde{\alpha}_k\right) \cdot \prod_{k=1}^{K}\Gamma(w_k)}{\Gamma(K) \cdot \prod_{k=1}^{K}\Gamma(\widetilde{\alpha}_k)}\right) + \\
+ \sum_{k=1}^{K}(\widetilde{\alpha}_k - w_k) \cdot \left[\psi(\widetilde{\alpha}_k) - \psi\left(\sum_{k=1}^{K}\widetilde{\alpha}_k\right)\right]
\end{aligned} \tag{5}
$$

With Γ being the gamma function, and ψ being the digamma function.

3.2 Uncertainty-Aware Attention Buffer for Knowledge Distillation

Prompt optimization involves minimizing a knowledge distillation loss $\mathcal{L}_{KD}$ term between the model attention maps (computed through attention rollout) and the maps available in our *uncertainty-aware attention buffer* A shared within all the C clients of the federation, with each client providing M attention maps for each of the K classes:

$$A = \bigcup_{c=1}^{C} \bigcup_{k=1}^{K} \bigcup_{m=1}^{M} a_{c,k,m} \qquad (6)$$

here $a_{c,k,i} \in \mathcal{R}^{H \times W}$ represents the ith attention map for the kth class of the cth client of the federation. H and W are the height and width of the attention maps equal to input image dimensions. The **knowledge distillation loss** $\mathcal{L}_{KD}$ for a generic training sample of client c, with class k can be expressed as:

$$\mathcal{L}_{KD} = \frac{1}{M} \sum_{i=1}^{C \backslash c} \sum_{m=1}^{M} \|a_{c,k,\_} - a_{i,k,m}\|^2 \qquad (7)$$

where, $\|a_{c,k,\_} - a_{i,k,m}\|^2$ denotes the squared Euclidean distance between the attention map $a_{c,k,\_}$ of the considered training sample and $a_{i,k,m}$ being an item of the buffer A.

The selection of samples for the attention buffer A by each client is based on the assumption that each local model should share its most confident predictions and indicate the image regions it focuses on. We use uncertainty scores from our evidential learning approach to guide the selection of attention maps for sharing within the federation. Specifically, we compute uncertainty scores, $u_j^{(k)}$, for each sample in class k, where j ranges from 1 to $N^{(k)}$, the total number of samples in class k. From these, we select the M samples with the lowest uncertainty scores, denoted as $\{u_1^{(k)}, u_2^{(k)}, \ldots, u_M^{(k)}\}$, and corresponding attention maps for inclusion in our uncertainty-aware attention buffer, A, replacing older ones.

4 Experimental results

We validate the effectiveness of our proposed method on a multicenter dataset of 23,247 dermoscopic images of nine skin lesions from different populations and medical centers, based on the ISIC2019 dataset Combalia et al. [2019], Codella et al. [2018], Tschandl et al. [2018]. To carry out federated learning, we organized the dataset into six nodes, with each node representing data from a specific source: Client C1 contains the BCN20000 dataset
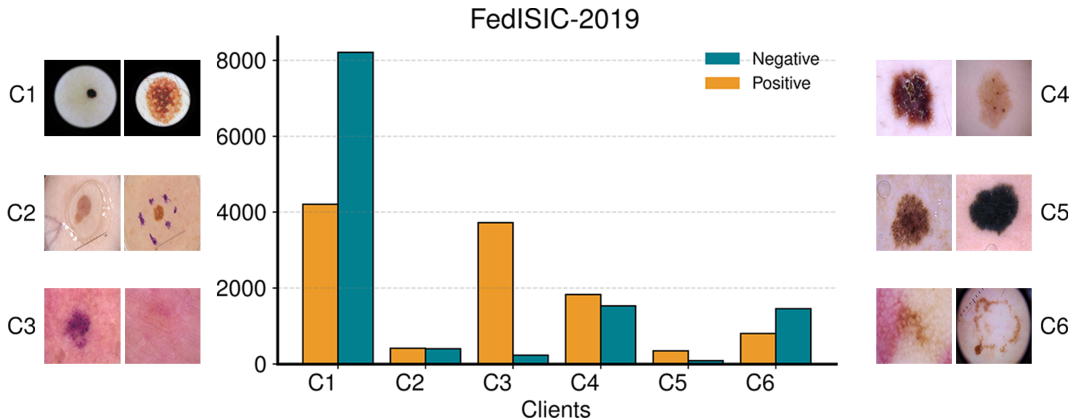

Figure 2: Distribution of the Fed-ISIC2019 dataset across clients.

as described by Combalia et al. Combalia et al. [2019], which includes 19,424 images from the Hospital Clínic in Barcelona; Clients C2, C3 and C4 are from the Austrian portion of the HAM10000 dataset Tschandl et al. [2018], with images from the ViDIR Group at the Department of Dermatology at the Medical University of Vienna; Client C5 is also part of the HAM10000 dataset and contains the Rosendahl image set from the University of Queensland in Australia; while client C6 includes the MSK4 dataset Codella et al. [2018]. The overall dataset

Table 1: **Comparison with state-of-the-art methods** on the Skin Lesion Dataset. In bold, best accuracy values.

	C1	C2	C3	C4	C5	C6	Avg
Local $b, t_{prompts}$	72.56	50.00	89.91	79.94	67.61	50.00	$68.34_{\pm 10.98}$
Local $g_{prompts}$	50.00	50.48	84.79	78.91	71.59	50.00	$64.30_{\pm 10.31}$
FedAvg[3]	74.74	72.79	67.74	79.89	67.61	77.09	$73.31_{\pm 3.64}$
FedAvgPers	77.79	68.01	84.84	78.08	67.61	82.66	$76.50_{\pm 7.25}$
FedProx[4]	81.34	68.14	74.69	75.15	77.84	78.65	$75.97_{\pm 4.55}$
FedProto[5]	71.88	69.04	66.34	69.71	58.52	73.57	$68.18_{\pm 5.34}$
FedDistill[6]	81.08	67.42	60.96	77.13	70.45	80.33	$72.90_{\pm 7.98}$
FedEvPrompt	81.02	71.83	84.15	79.02	68.18	79.35	$\mathbf{77.26}_{\pm 4.65}$

exhibits heterogeneity in both the number of images contributed by each client as well ass in the distribution of classes, as illustrated in Fig. 2, making it a strong real-world use case for testing federated learning methods. For this study, we will focus on the binary classification task of distinguishing *Melanocytic nevus* from other skin lesions.

Training procedure In our setup, for each client, data is divided into a 75% training and 25% test split. Training is executed over 5 communication rounds, with 15 training epochs per round. Our model architecture employs a frozen ViT backbone augmented with additional parameters for b-prompts, t-prompts, and a classification-head. The ViT backbone specifications include an embedding dimension of 384, 6 attention heads, 12 blocks, and an input size of 224x224 pixels. For the b-prompts and t-prompts, the prompt keys (k and v) have a sequence length of 50, while l is 3 out of the 12 attention layers. We set the learning rates μ_1 and μ_2 to $2.5e-4$ and $5e-4$ respectively, with a weight decay factor of $1e-2$. Additionally, each client contributes 5 attention rollout maps per class (i.e., M in Eq. 6) to the uncertainty-aware attention buffer. Results are presented as in terms of balanced accuracy on the test set at the conclusion of all rounds.

Results. In Table 1, we present a comprehensive performance comparison between FedEvPrompt and existing federated learning methods. FedAvg McMahan et al. [2017] serves as our baseline. FedAvgPers builds upon FedAvg by integrating a personalization step through local data fine-tuning, aligning with our emphasis on personalized learning via b-prompts and t-prompts tuning. Additionally, we incorporate FedProx Li et al. [2020], specifically tailored to address non-IID data like our skin lesion dataset.

Given that our approach employs knowledge distillation without parameter sharing, we include two analogous methods in our analysis: FedProto Tan et al. [2022] and FedDistill Seo et al. [2022]. We also evaluate the performance of local training, where client models are trained independently without parameter sharing, using both sets of prompts (i.e., $(b, t)_{prompts}$), and using only one set of prompts ($g_{prompts}$ - general prompts) across all attention layers. We define g-prompts $= [b$-prompts, t-prompts$]$ with both learning rates set to μ_1. This evaluation aims to validate our choice to apply different parameters across different attention layers and to demonstrate the advantages provided by our federated learning approach.

Results show that FedEvPrompt outperforms its competitors, including those that share parameters (thus being less privacy-preserving), such as FedAvg McMahan et al. [2017] and FedProx Li et al. [2020]. Notably, when comparing FedEvPrompt performance with other methods that do not share parameters, namely FedProto Tan et al. [2022] and FedDistill Seo et al. [2022], we observe higher performance across all clients and a lower standard deviation, indicating better convergence in accuracy among clients.

We finally conducted an ablation study to assess the impact of various prompting options and sharing strategies among nodes within the federation. It's worth noting that while prompt sharing may potentially compromise privacy guarantees, exploring its effectiveness compared to using private prompts and our proposed knowledge distillation approach is interesting.

To this end, we initially assessed the performance of a variant of FedAvg where only low-level *b-prompts* are shared, gradually incorporating *t-prompts* and knowledge distillation on the uncertainty-aware attention buffer. Furthermore, we examined the variant of the proposed prompting strategy using a single set of general prompts *g-prompts* shared between nodes and coupled with our knowledge distillation method. Our findings, outlined in Table 2, underscore the significance of separate prompt learning, as evidenced by the subpar performance of the *g-prompts* variants. Interestingly, sharing separate sets of *b-prompts* and *t-prompts* (first two rows of Tab. 2) proved less effective than keeping them private and employing knowledge distillation (best performance observed in the last two rows of the same table). Moreover, we demonstrate that our strategy of incorporating attention maps based on uncertainty scores (as detailed in Sect. 3.2) yields superior performance compared to random selection of buffer samples. These two last considerations highlight

Table 2: **Ablation study results** showing the impact of shared prompts and knowledge distillation (KD) on federated learning performance.

	C1	C2	C3	C4	C5	C6	Avg
FedAvg $b_{prompts}$	50.00	70.04	70.29	79.61	71.59	79.21	$70.18_{\pm 7.56}$
+ $t_{prompts}$	74.74	72.79	67.74	79.89	67.61	77.09	$73.31_{\pm 3.64}$
+ KD	73.02	71.41	76.80	81.74	67.61	79.25	$74.97_{\pm 3.94}$
FedAvg $g_{prompts}$	50.00	70.88	72.77	50.00	67.61	50.00	$60.21_{\pm 6.81}$
FedAvg $g_{prompts}$ + KD	81.1	71.32	72.83	78.89	63.64	80.49	$74.71_{\pm 6.18}$
KD$_{random}$	78.12	69.40	76.80	80.30	68.75	77.65	$75.17_{\pm 3.66}$
KD$_{uncertainty}$ *(Ours)*	81.02	71.83	84.15	79.02	68.18	79.35	$\mathbf{77.26}_{\pm 4.65}$

the informative contribution provided by the attention maps corresponding to the lowest uncertainty samples driving clients' models towards the most significant regions of skin lesion images.

5 Conclusion

This work introduces FedEvPrompt, a new federated learning approach tailored for skin lesion classification using the ISIC2019 dataset. Indeed, this dataset offers a realistic setting for evaluating federated learning methods, eliminating the need for simulated distributions. FedEvPrompt seamlessly integrates evidential deep learning, prompt tuning, and knowledge distillation within a vision transformer architecture. Knowledge distillation on attention maps, in particular, ensures better privacy-preserving capabilities than parameter sharing. In addition to its superior performance in addressing data heterogeneity and privacy concerns, the employment of evidential learning offers enhanced model interpretability and uncertainty quantification, providing valuable insights for decision-making in medical image analysis. Balancing vacuity and dissonance Josang et al. [2018], Guo et al. [2022] in buffer selection warrants further research to comprehensively understand underlying mechanisms.

Acknowledgements

References

Brendan McMahan et al. Communication-efficient learning of deep networks from decentralized data. In *Artificial intelligence and statistics*, pages 1273–1282. PMLR, 2017.

Tian Li, Anit Kumar Sahu, Manzil Zaheer, Maziar Sanjabi, Ameet Talwalkar, and Virginia Smith. Federated optimization in heterogeneous networks. *Proceedings of Machine Learning and Systems*, 2:429–450, 2020.

Murat Sensoy, Lance Kaplan, and Melih Kandemir. Evidential deep learning to quantify classification uncertainty. *Advances in neural information processing systems*, 31, 2018a.

Meng Wang, Lianyu Wang, Xinxing Xu, Ke Zou, Yiming Qian, Rick Siow Mong Goh, Yong Liu, and Huazhu Fu. Federated uncertainty-aware aggregation for fundus diabetic retinopathy staging. *arXiv preprint arXiv:2303.13033*, 2023.

Xiang Lisa Li and Percy Liang. Prefix-tuning: Optimizing continuous prompts for generation. *arXiv preprint arXiv:2101.00190*, 2021.

Guanghao Li, Wansen Wu, Yan Sun, Li Shen, Baoyuan Wu, and Dacheng Tao. Visual prompt based personalized federated learning. *arXiv preprint arXiv:2303.08678*, 2023.

Yifu Zhang, Zuozhu Liu, Yang Feng, and Renjing Xu. 3d-u-sam network for few-shot tooth segmentation in cbct images. *arXiv preprint arXiv:2309.11015*, 2023.

Jonas Geiping, Hartmut Bauermeister, Hannah Dröge, and Michael Moeller. Inverting gradients-how easy is it to break privacy in federated learning? *Advances in Neural Information Processing Systems*, 33:16937–16947, 2020.

Ligeng Zhu, Zhijian Liu, and Song Han. Deep leakage from gradients. *Advances in neural information processing systems*, 32, 2019.

Matteo Pennisi, Federica Proietto Salanitri, Giovanni Bellitto, Bruno Casella, Marco Aldinucci, Simone Palazzo, and Concetto Spampinato. Feder: Federated learning through experience replay and privacy-preserving data synthesis. *Computer Vision and Image Understanding*, 238:103882, 2024.

Hyowoon Seo, Jihong Park, Seungeun Oh, Mehdi Bennis, and Seong-Lyun Kim. Federated knowledge distillation. *Machine Learning and Wireless Communications*, page 457, 2022.

Yue Tan, Guodong Long, Lu Liu, Tianyi Zhou, Qinghua Lu, Jing Jiang, and Chengqi Zhang. Fedproto: Federated prototype learning across heterogeneous clients. In *Proceedings of the AAAI Conference on Artificial Intelligence*, volume 36, pages 8432–8440, 2022.

Niclas Ståhl, Göran Falkman, Alexander Karlsson, and Gunnar Mathiason. Evaluation of uncertainty quantification in deep learning. In *International Conference on Information Processing and Management of Uncertainty in Knowledge-Based Systems*, pages 556–568. Springer, 2020.

Murat Sensoy, Lance Kaplan, and Melih Kandemir. Evidential deep learning to quantify classification uncertainty. In S. Bengio, H. Wallach, H. Larochelle, K. Grauman, N. Cesa-Bianchi, and R. Garnett, editors, *Advances in Neural Information Processing Systems*, volume 31. Curran Associates, Inc., 2018b. URL `https://proceedings.neurips.cc/paper_files/paper/2018/file/a981f2b708044d6fb4a71a1463242520-Paper.pdf`.

Samira Abnar and Willem Zuidema. Quantifying attention flow in transformers. *arXiv preprint arXiv:2005.00928*, 2020.

JoramSoch(2021). Proof:. Kullback-leibler divergence for the dirichlet distribution. `https://statproofbook.github.io/P/dir-kl.html` ; DOI:10.5281/zenodo.4305949.

Marc Combalia, Noel C. F. Codella, Veronica Rotemberg, Brian Helba, Veronica Vilaplana, Ofer Reiter, Cristina Carrera, Alicia Barreiro, Allan C. Halpern, Susana Puig, and Josep Malvehy. Bcn20000: Dermoscopic lesions in the wild, 2019.

Noel CF Codella, David Gutman, M Emre Celebi, Brian Helba, Michael A Marchetti, Stephen W Dusza, Aadi Kalloo, Konstantinos Liopyris, Nabin Mishra, Harald Kittler, et al. Skin lesion analysis toward melanoma detection: A challenge at the 2017 international symposium on biomedical imaging (isbi), hosted by the international skin imaging collaboration (isic). In *2018 IEEE 15th international symposium on biomedical imaging (ISBI 2018)*, pages 168–172. IEEE, 2018.

Philipp Tschandl, Cliff Rosendahl, and Harald Kittler. The ham10000 dataset, a large collection of multi-source dermatoscopic images of common pigmented skin lesions. *Scientific data*, 5(1):1–9, 2018.

Audun Josang, Jin-Hee Cho, and Feng Chen. Uncertainty characteristics of subjective opinions. In *2018 21st International Conference on Information Fusion (FUSION)*, pages 1998–2005. IEEE, 2018.

Zhen Guo, Zelin Wan, Qisheng Zhang, Xujiang Zhao, Feng Chen, Jin-Hee Cho, Qi Zhang, Lance M Kaplan, Dong H Jeong, and Audun Jøsang. A survey on uncertainty reasoning and quantification for decision making: Belief theory meets deep learning. *arXiv preprint arXiv:2206.05675*, 2022.